


Research Article

Porous Blasting Morphology and Resistivity Response Characteristics of Soft Coal Seam

Wenwang Yang,^{1,2} Sanlin He ,³ Taotao Zhao,⁴ and Chenying Ge^{1,2}

¹School of Safety Science and Engineering, Anhui University of Science and Technology, Huainan 232001, China

²National and Local Joint Engineering Research Center for Precise Mining of Coal Safety, Anhui University of Science and Technology, Huainan 232001, China

³Human Resources Office, Anhui University of Science and Technology, Huainan 232001, China

⁴Beijing Enterprises Water Group Limited, Beijing 100102, China

Correspondence should be addressed to Sanlin He; wwyang@aust.edu.cn

Received 10 May 2022; Revised 13 July 2022; Accepted 19 July 2022; Published 12 August 2022

Academic Editor: Antonio Giuffrida

Copyright © 2022 Wenwang Yang et al. This is an open access article distributed under the Creative Commons Attribution License, which permits unrestricted use, distribution, and reproduction in any medium, provided the original work is properly cited.

The fracturing characteristics of multi-holes blasting in soft coal seam were analyzed quantitatively by using the multi-holes model blasting experiment of soft coal seam and digital image processing (DIP) and electrical resistivity tomography (ERT) techniques, and the electrical resistivity response rules before and after blasting were obtained. The results show the following: (1) At the same time as the formation of blasting-induced cracks, the coal inside the control hole presents two kinds of displacement phenomena: crack and noncrack, partially offsetting the extrusion effect caused by the expansion of the blasting hole. (2) The comprehensive value (S) of blasting-induced cracks, control hole, and blasting hole area change is proposed to analyze the blasting effect. When single-hole blasting is performed, $S < 0$, the fractal dimension change rate of coal seam crack is only 5%, the control area presents a compaction phenomenon, and the resistivity decreases by about 20%. When multi-hole blasting is performed, the blasting cracks are abundant and the coal displaces sufficiently. The fractal dimension of cracks reaches 21.28%, the negative effect of the blast holes cavity is offset ($S > 0$), and the resistivity in the controlled area generally increases by 1 to 30 times. (3) Compared with the single-hole blasting model, the multi-hole blasting is more in line with the coal mine site, and can effectively increase the permeability in the control area, and the resistivity generally increases.

1. Introduction

The soft coal seam is the product of geological structure and is widely distributed in China [1]. Soft coal seam has the typical characteristics of low strength, low permeability, loose coal quality, and so on, and the effect of gas extraction is poor, which seriously restricts mine safety production [2, 3].

Deep-hole presplit blasting can make full use of explosive energy and the guiding function of the control hole by arranging blasting holes and control holes in the coal seam, to produce blasting crack in the control area and provide passage for gas migration [4]. Deep-hole presplit blasting technology has been widely used in low permeability

coal seams, and various blasting methods have gradually developed such as directional shaped blasting [5], water pressure blasting [6], and slot water pressure blasting [7], with great development in charge and coupling form [8–11].

The formation and morphology of explosion crack are the results of the combined action of explosion shock wave and explosion gas [12–16]. When the shock wave acts on the coal wall, its pressure far exceeds the dynamic tensile strength of the coal, and the coal is destroyed to form a crushing zone [12, 13]. Then the shock wave decays into a stress wave and spreads to a distance. Under the action of compressive stress and tensile stress respectively, the coal breaks and forms cracks [14, 15]. The explosive gas has a quasi-static gas wedge effect on the crack, which can prolong

TABLE 1: Model-making scheme.

Layering of models	The ratio of different materials					Compressive strength (MPa)
	Sand	Cement	Gypsum	Coal powder	Water	
1 # rock	5.6	1.0	2.0	0	2.1	9.27
Coal	3.5	0.3	1.0	1.0	1.37	0.45
2 # rock	5.2	1.0	2.5	0	2.1	10.16

the crack propagation length and increase the stress peak of the medium in the elastic vibration zone [16]. The explosion wave has a greater impact on the high impedance rock mass, and the expansion pressure of explosion gas has a greater impact on low impedance rock mass [17].

When the stress wave propagates to the control hole wall, it is reflected, and the reflected tensile wave and the stress field at the radial crack tip are superimposed on each other to promote crack expansion. When the crack expands near the control hole, the dynamic stress intensity factor of the main crack tip increases, which makes it play the role of energy gathering and guiding and controlling the crack in the blasting process [18, 19]. Blasting crack surface appears along the core line of blasting hole and control hole, which is proved by theoretical research and field engineering practice.

The shape of the coal blasting crack is closely related to its strength. With the increase of coal strength, the crack zone and plastic zone decrease correspondingly [20, 21]. As the coal is a soft porous medium, most of the explosion energy is absorbed in the near zone, forming a large compression crack zone around the charge column, but the plastic zone is much smaller. This is also the reason why gas extraction efficiency is high in the short term after deep-hole presplit blasting, but its attenuation is fast [14].

In the field of deep-hole presplit blasting, great achievements have been made, but there are some shortcomings. Especially for the soft coal with low strength, most of the previous studies focused on the morphological characteristics of the explosion crack, ignoring the changes in coal displacement and borehole. In addition, in coal mine antireflection work, a single blasting hole is seldom used, but many control holes and blasting holes are arranged at the same time, which is neglected in the present research.

Therefore, this paper carried out the porous model blasting experiment of the soft coal seam and obtained the crack morphology of the soft coal seam and the regional resistivity variation rule of coal during porous blasting by using DIP and resistivity tomography technology (ERT).

2. Experimental Model and Scheme

2.1. Experimental Model. To simulate the actual occurrence state of coal strata, a three-layer physical model including rock mass and coal was adopted in the experiment. According to the actual strength of coal seam, roof, and floor rock strata in the uncovering coal area of the north section of 25091 working face of Henan Gaocheng Coal Mine, the coal and rock mass are allocated with sand, cement, gypsum, coal powder and water in different proportions. The allocation of

rock mass and coal is shown in Table 1. The blasting model is established by layering, and each layer must be fully dried. Before the model is laid, the experimental frame is insulated to ensure the accuracy of the signal collected by the electric analyzer. After the model was established, it was left to rest for 28 days.

The size of the experimental model is 72 cm × 72 cm × 35 cm, a vertical load of 2.5 MPa can be applied, and rigid constraints can be carried out around the model, to avoid or reduce the blasting debris at the model boundary [22], as shown in Figure 1. In the matching scheme, the compressive strength of rock mass and coal is different, which can well simulate the occurrence state of the soft coal seam. The thickness of the coal seam is 10 cm, and the thickness of the roof and floor are 12.5 cm. After laying coal, a ring of electrodes was arranged around the coal, 64 in total, as shown in Figure 2. The length of the electrode is 2.4 cm nails, wire enameled wire. Before using the electrodes, apply the conductive paste evenly on the surface of the nails, and then insert it into the model successively.

The experimental model was set up with 1, 2, and 4 blasting holes, and 4, 6, and 9 control holes, respectively, to ensure that the blasting holes were in the center of the 4 control holes, as shown in Figure 3. The hole diameter of the blasting hole is 9 mm and the depth is 225 mm.

Relevant studies show that the larger the control hole diameter is, the larger the free space for blasting is, and the better the blasting cracking effect is. Therefore, to better study the cracking and deformation characteristics of soft coal seam after blasting, a large diameter control hole ($\phi 50$ mm) was adopted in the experiment (the diameter of the drilling hole was enlarged by using hydraulic punching or cutting in the project). The center distance between the control hole and the blasting hole is 150 mm. The number and aperture of each borehole are shown in Table 2.

2.2. The Experimental Scheme. RDX explosive was used for blasting, with a charge volume of 1.2 g and length of 10 cm. The sealing hole section is located in the rock formation, and the sealing hole length is 12.5 cm. A special detonator was used for remote initiation, as shown in Figure 4. The blasting experiment was carried out at the blasting site of Anhui University of Science and Technology.

30 min before blasting, the YBD network parallel electrical analyzer was used to collect signals, and the resistivity distribution of the coal seam before blasting was inverted. 30 min after blasting, the signal is collected again to obtain the resistivity distribution of the coal seam. After the signal collection, the model was opened to observe and photograph the shape of the crack. The crack width was measured by

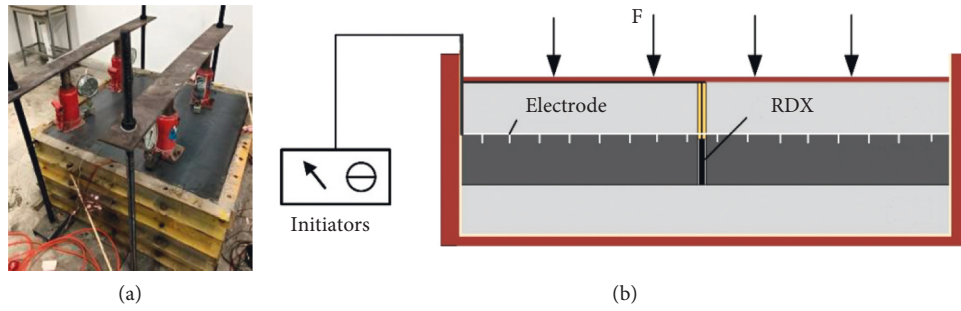


FIGURE 1: The experimental system. (a) Prepared model. (b) Experimental model diagram.

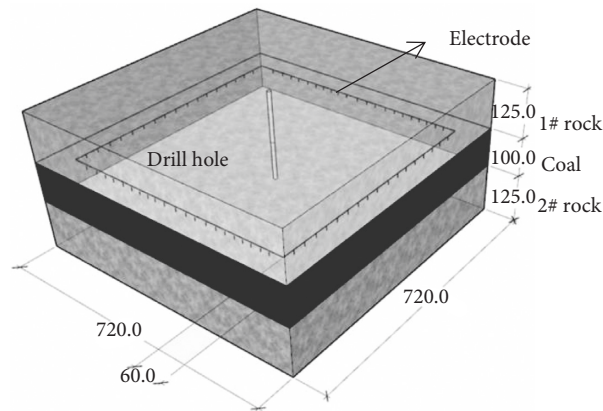


FIGURE 2: Electrode position distribution (unit: mm).

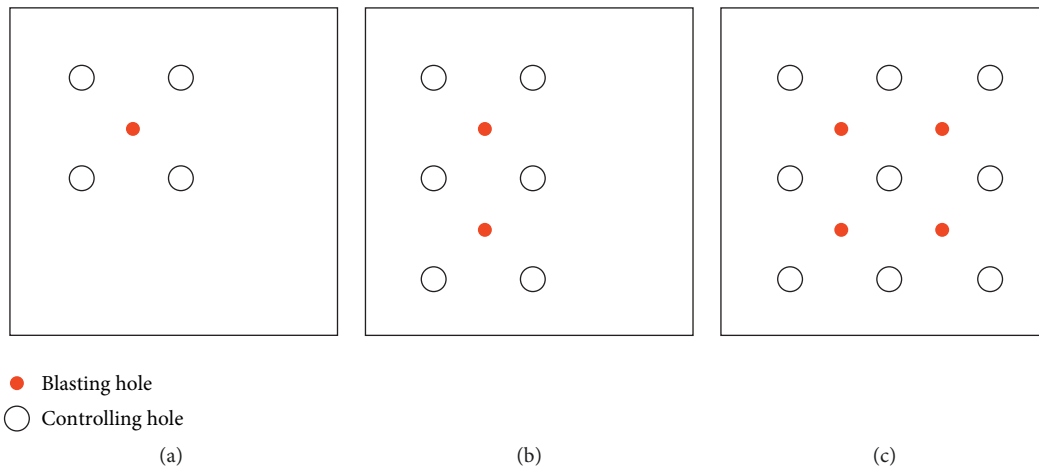


FIGURE 3: The blasting models. (a) Single-hole blasting model. (b) Double-hole blasting model. (c) Four-hole blasting model.

TABLE 2: Drilling parameters.

Drilling type	Diameter/mm	Mode of blasting	Number
The blasting hole	9	Single hole	DB-#
		Double hole	LB-#
		Four hole	SB-#
The control hole	50	Single hole	DK-#
		Double hole	LK-#
		Four hole	SK-#



FIGURE 4: Blasting device. (a) RDX. (b) Initiators.

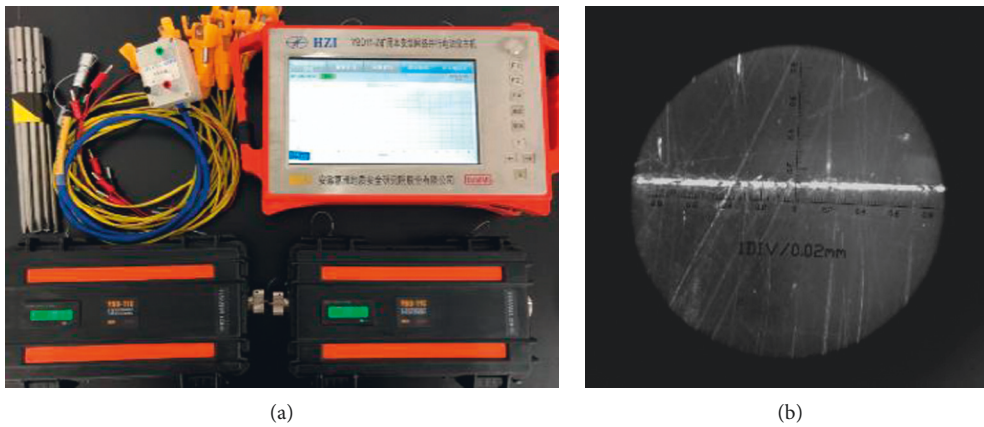


FIGURE 5: Data acquisition equipment. (a) YBD network parallels electrometer. (b) MG10085-1A 100 reading microscope.

MG10085-1A 100 reading microscope, and the grayscale map of the coal seam surface crack was processed using Matlab software, and then the crack area was calculated using AutoCAD software. The equipment is shown in Figure 5. Specific steps are shown in Figure 6.

3. Crack Morphology of Porous Blasting

3.1. Cracking Morphology of Soft Coal. The area surrounded by the line of the center of the control hole is called the control area. After the explosion of the charge column, there are three typical crack formation patterns in the control area, that is, the expansion of the blasting hole, the formation of the explosion crack, and the reduction of the control hole, while outside the control area, only the formation of the explosion crack occurs, as shown in Figure 7.

- (1) Blasting hole expansion. The explosion of the charge column produces pulverizing zone near the borehole and destroys the coal structure. Under the action of blasting dynamic pressure and explosive gas expansion pressure, the blasting hole expands and its aperture reaches 3–10 times the original state. However, the expansion of the blasting hole will cause the surrounding coal to be squeezed and the gas flow channel to be closed, so the expansion of the

blasting hole harms reflection enhancement in the control area.

- (2) Explosion crack. The generation of cracks provides gas flow channels and has a positive effect on antireflection. However, the coal on both sides of the crack plane may be squeezed due to space demand from the surrounding coal.
- (3) Control hole reduced. The coal displaces and fills part of the control hole. The decrease of the control hole area provides space for the porosity of coal in the control area, which has a positive effect on antireflection.

3.2. Coal Displacement Phenomenon. The strength of coal is low, and the coal between the blasting hole and the control hole is displaced by the blasting dynamic pressure and presents two displacement modes of crack and noncrack.

When the local coal and the surrounding coal are completely fractured, the separated “fractured coal” moves, which can also be called the “moving body”. In the double-hole blasting model, the coal deformation inside the control holes LK-1 and LK-5 belong to this category, as shown in Figure 8 Radial cracks appear on the side of the “moving body” and tangential cracks appear on the rear end cut-off

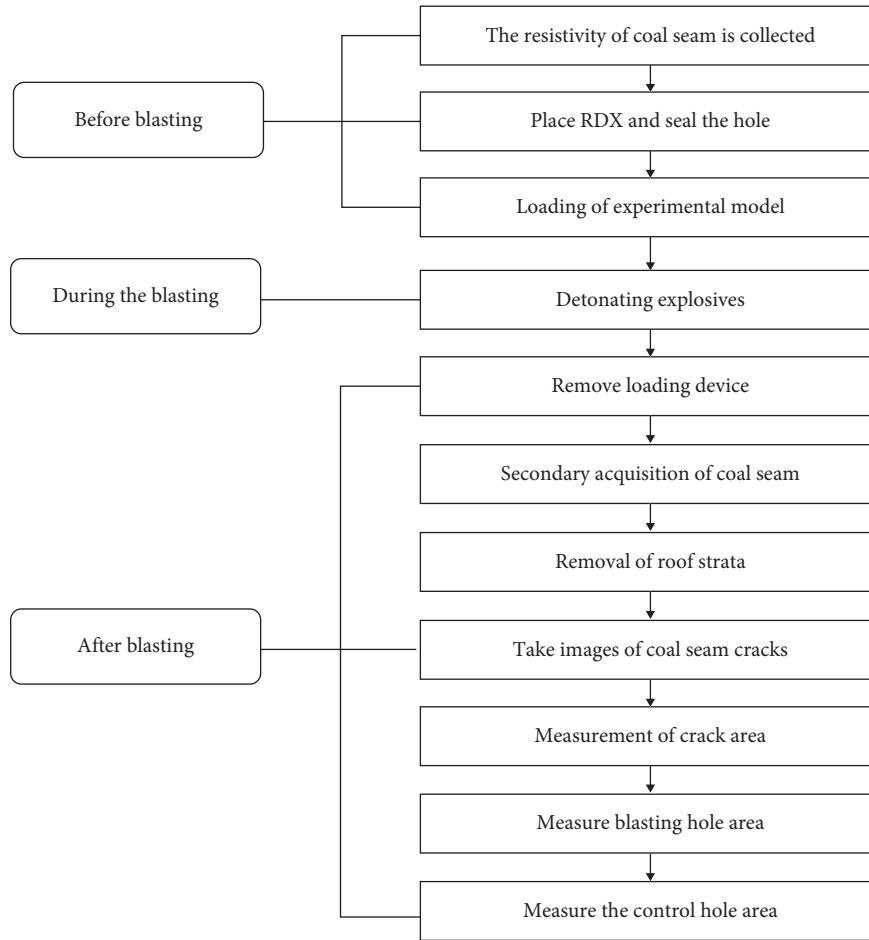


FIGURE 6: The experimental steps.

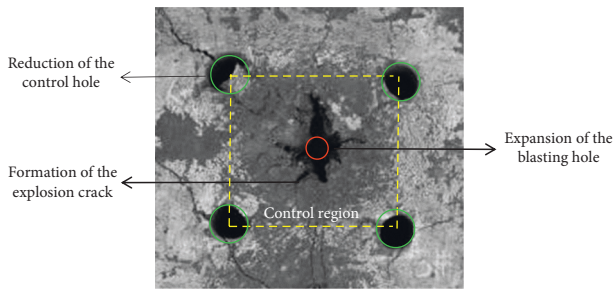


FIGURE 7: Crack morphology of soft coal (Single-hole blasting model).

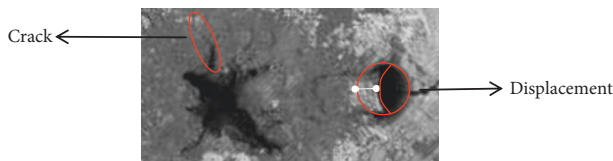


FIGURE 8: Deformation of coal inside control holes.

the moving body and moved towards the control hole, partially filling the control hole. Because the moving body has broken with the surrounding coal, the displacement is large and the control hole is well filled.

When the moving coal does not completely crack with the surrounding coal seam, it is called noncrack displacement, and most of the coal movement in the model belongs to this type. Under the action of blasting dynamic pressure, the coal moves as a whole, and the control hole is partially filled. Compared with the former, the noncrack displacement is much smaller. The displacement of the moving body is taken as the filling length of the filling of the control borehole along the center line, and then all the displacement of the control borehole is obtained. The original area of the control hole was 19.6 cm^2 , and that of the blasting hole was 0.64 cm^2 . This paper adopts a plane area to analyze the spatial changes of cracks, as shown in Figure 9.

Although the control holes are evenly arranged around the blasting holes, the displacement of each hole is different. In the single-hole blasting model, the filling amount of DK-1 and DK-2 control holes are small, and the displacement of coal is $0.51 \sim 0.57 \text{ cm}$. In the double-hole blasting model, only the LK-6 hole did not appear filling phenomenon, and the coal displacement of other control holes ranged from 0.52 cm to 1.88 cm , and the maximum displacement appeared in the inner side of the LK-1 hole. In the four-hole blasting model, all the control holes are filled to different degrees, and the displacement of coal is $0.2 \sim 1.08 \text{ cm}$.

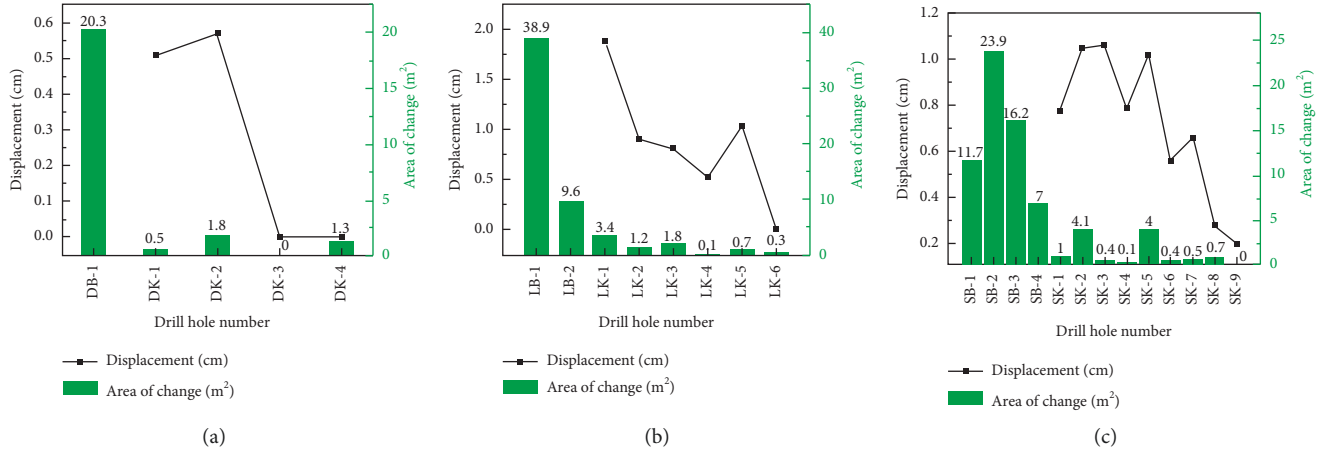


FIGURE 9: Change of drilling displacement and area after blasting. (a) Single-hole blasting model. (b) Double-hole blasting model. (c) Four-hole blasting model.

With the increase in the number of blasting holes, the coal deformation in the control area tends to be uniform, and the control hole space decreases, which provides conditions for the regional loosening of coal.

3.3. Characteristics of Explosion Crack. To analyze the morphological characteristics of cracks, the width and fractal dimension of cracks were compared quantitatively, as shown in Figure 10.

3.3.1. Crack Width. With the increase in the number of blasting holes, the width of the blasting crack also increases. In the control area, the crack width of the single-hole blasting model is 0.1–1.2 mm, and the maximum crack width is 1.0–1.2 mm at the coal displacement inside the control hole DK-1. The width of the crack in the double-hole blasting model is 0.3~3.5 mm, and the maximum width of the crack is 3.5 mm inside the control hole. In the four-hole blasting model, the width of the crack is 0.6~3.4 mm, and the maximum width of the crack also appears on the inner side of the control hole, which is 3.4 mm.

In the control area, the maximum width of the crack appears at the coal displacement measured in the control hole, and the larger the coal displacement is, the larger the crack width is. In the single-hole blasting model, the deformation of hole DK-1 reaches 5.1 mm, and the crack width is the largest (1.2 mm). In the double-hole blasting model, the deformation of the LK-1 hole reaches 18.8 mm, and the width of the crack inside the control hole reaches 1.6–1.8 mm, but the lateral crack is wider (0.9~3.5 mm). In the model of four blasting holes, the deformation of the SK-4 hole is 8 mm, but due to the superposition of adjacent blasting, the width of cracks inside the control hole is 2.6~3.4 mm, and the width of cracks outside is 0.5~1.5 mm.

3.3.2. Fractal Dimension of Crack. Blasting coal seam gap caused by the process of evolution is a process of a fractal, fractal dimension is a can show the characteristics of blasting result in crack evolution degree, the shape variation of

applying fractal geometry to the blasting of research [23, 24], will deepen the understanding of critical raw fracture morphology, especially after using fractal dimension characterization of blasting crack of quantitative analysis [25, 26]. To a certain extent, the problem of the irregular distribution of cracks after blasting is solved.

In this section, the fractal theory is used to study the geometric distribution of coal seam cracks and determine their fractal dimension, to quantitatively compare and analyze the explosion cracks under different models. The crack images under different blasting models are processed to obtain the corresponding gray image, the gray image is binarized, the mesh division and statistics are carried out, and then the box dimension of the explosion crack is obtained [27, 28].

According to the box dimension theory, the box dimension of any nonempty bounded target set X in space Rn is

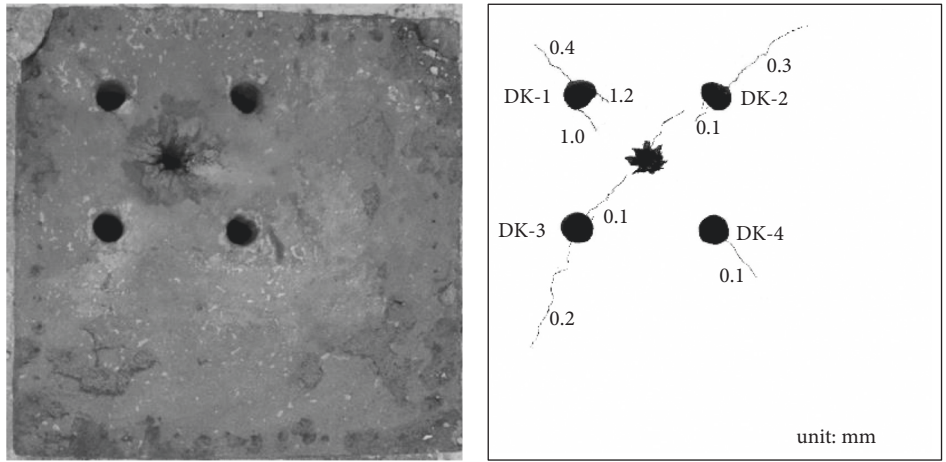
$$D = \frac{-\lim_{k \rightarrow \infty} \lg N_{\delta_k}(X)}{\lg \delta_k}. \quad (1)$$

In this formula: Rn is the space of dimension N , δ_k is the established descending sequence based on the size of the square box, $N_{\delta_k}(X)$ is the minimum number of grids required to cover the target set X with a square box of size δ_k .

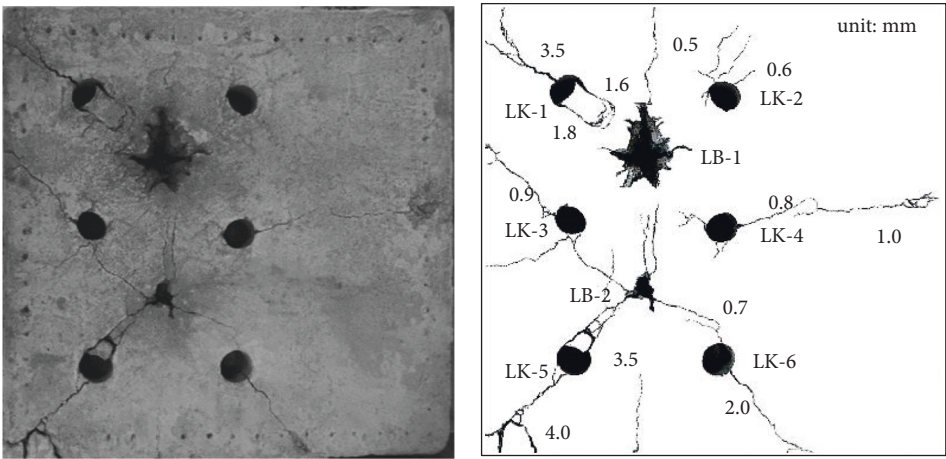
Firstly, the fractal dimension of the coal seam surface with drilling before blasting is calculated, and the initial fractal dimension D_0 is obtained. Then, the fractal dimension of surface morphology with blasting crack is calculated and D_1 is obtained. The two are subtracted to obtain the fractal dimension of coal seam surface crack change ΔD , as shown in Table 3. With the increase in the number of blasting holes, the change rate of fractal dimension of coal seam crack (displacement of coal) increases, and the coal seam crack tends to be complicated.

4. Comprehensive Evaluation of Coal Blasting Deformation

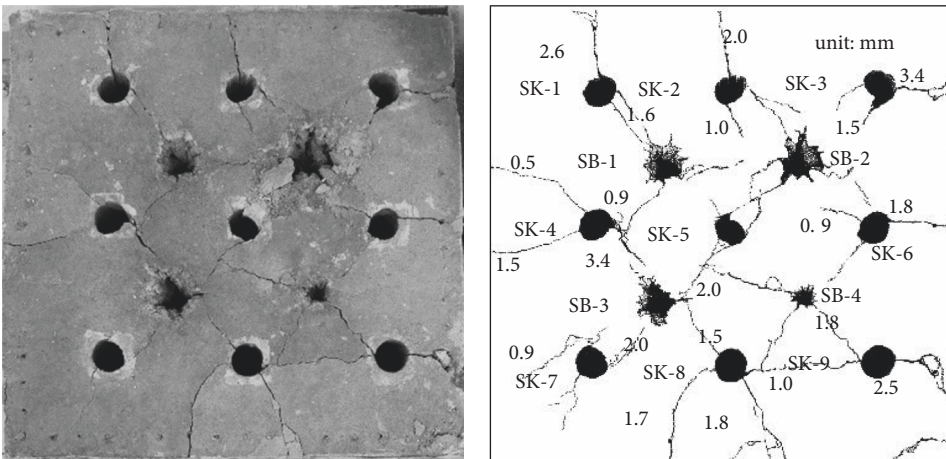
4.1. Comprehensive Evaluation of Coal Deformation. After the bursting of the soft coal, three typical crack morphology on the antireflection effect is different, for the function of



(a)



(b)



(c)

FIGURE 10: Crack morphology and resistivity distribution diagram after blasting. (a) Single-hole blasting model. (b) Double-hole blasting model. (c) Four-hole blasting model.

TABLE 3: Calculation results of crack fractal dimension.

Model	Initial fractal dimension D_0	Fractal dimension after blasting D_1	Change in fractal dimension ΔD	$\Delta D/D_0$ (%)
Single-hole blasting	1.041	1.093	0.052	5.00
Two blasting	1.026	1.235	0.209	20.37
Four-hole blasting	1.015	1.231	0.216	21.28

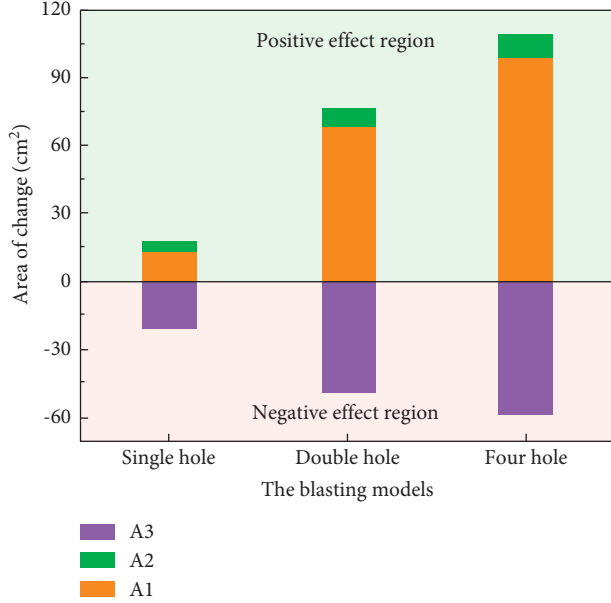


FIGURE 11: Analysis of permeability variation.

comprehensive evaluation. In this paper, the comprehensive change (S) of the area of the crack, control hole, and blasting hole is used to analyze the blasting effect. The crack area A_1 and the control hole reduced area A_2 were taken as the evaluation value of the positive reflection improvement effect. The increase of blasting hole area A_3 is taken as the evaluation value of the negative reflection improvement effect, that is, $S = A_1 + A_2 - A_3$. The result is shown in Figure 11.

- (1) Single-hole blasting model. In the control area, although the surface crack of the coal seam is obvious, the total deformation of the control hole is small. The expansion area of the blasting hole is much larger than the decreased value of the control hole, and the blasting action compacts the coal in the control area. The control hole deformation space is difficult to offset the compaction effect, so the overall antireflection effect is negative. Outside the control area, the explosion crack shows a positive effect.
- (2) Double-hole blasting model. In the control area, the total expansion area of the two blasting holes is 2.4 times that of the single-hole blasting, which has a great compaction effect on coal. However, the area of the new crack and reduced area of the control hole are 5.2 times and 2.1 times that of single-hole blasting respectively, which effectively

offset the expansion and compaction effect of blasting hole. Outside the control area, the area of detonation crack is 7.8 times that of single-hole blasting, which effectively realizes the antireflection outside the control area.

- (3) Four-hole blasting model. Similar to the double-hole blasting model, the area of the new crack and the reduced area of the control hole in the control area effectively offset the expansion and compaction effect of the blasting hole, so that the blasting antireflection effect presents a positive effect. Outside the control area, the area of detonation crack is 17.3 times that of single-hole blasting, which effectively realizes the antireflection outside the control area.

4.2. Regional Resistivity Response of Coal. Resistivity information can reflect the changes in coal and rock cracks [29–31], which can be used to analyze the damage characteristics of the coal seam. The network parallels the electrical method can realize the full electric field observation, through the extraction of effective signals, effective data encoding, and two-dimensional or three-dimensional resistivity tomography. In this paper, a two-dimensional resistivity imaging method was adopted to obtain the resistivity multiple distributions before and after blasting, as shown in Figure 12. Resistivity change before and after blasting $\Delta\rho$ is

$$\Delta\rho = \frac{\rho_2}{\rho_1}. \quad (2)$$

In the formula, ρ_1 is the resistivity before blasting ρ_2 is the resistivity after blasting. When $\Delta\rho > 1$ it shows an increase in resistivity; when $\Delta\rho < 1$ it shows a decrease in resistivity.

The larger the change multiple is, the greater the change degree of resistivity is after blasting, and the more serious the damage to coal is. When the change multiple is less than 1, the resistivity decreases and the coal may be partially compacted.

4.2.1. Single-Hole Blasting Model. Corresponding to the analysis results in Section 4.1, in the single-hole blasting model, $S < 0$, the occurrence of cracks not only does not cause large area damage to the control area, but compacts the surrounding coal, reducing the resistivity by 20%, and presenting the overall resistivity reduction phenomenon in the control area.

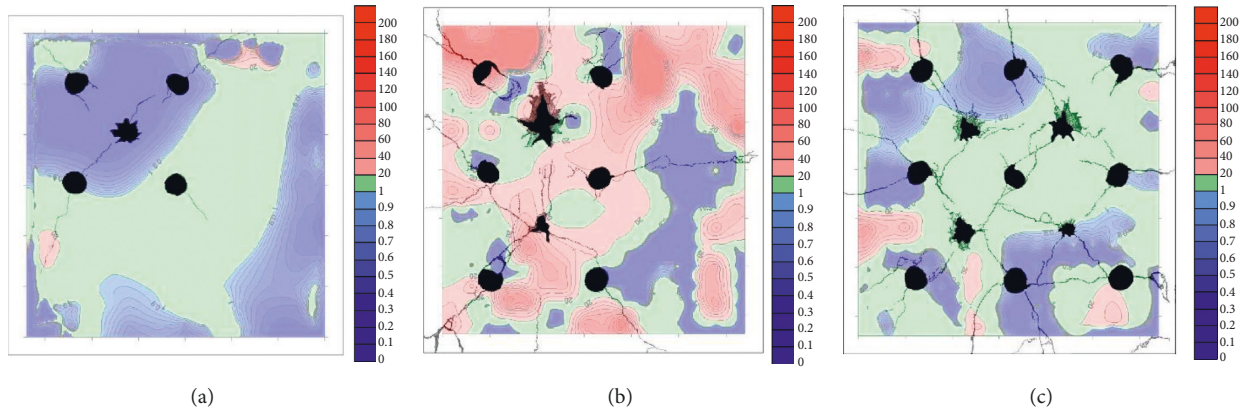


FIGURE 12: Crack and electrical resistivity after blasting. (a) Single-hole blasting model. (b) Double-hole blasting model. (c) Four-hole blasting model.

Outside the control area, on the one hand, the damage is formed in the far area due to stress wave compression and unloading, and the emergence of an explosion crack outside the control hole causes damage to the coal, which leads to the phenomenon that the resistivity outside the control area increases instead, can be increased up to 20 times. Due to the rigid constraints around the model, local extrusion will occur near the edge of the model, and the resistivity will decrease.

4.2.2. Double-Hole Blasting Model. The crack of the double-hole blasting model is better than that of the single-hole blasting model, and the resistivity increases up to 50 times in the control area. Due to the formation of crack space, cracks are squeezed on both sides and compaction still occurs in local areas, which leads to the reduction of local resistivity, as shown in Figure 12(b), by about 10%–20%.

Although a long crack was formed on the lateral side of LK-4, the crack squeezed the coal on both sides of the crack plane at the same time, which reduced the resistivity. The resistivity increase of the outer side of the control hole was significantly higher than that of the inner side, such as the outer side of the drilling LK-1 and LK-4, which reached 200 times, while the inner resistivity is only 40 times as high as the original.

4.2.3. Four-Hole Blasting Model. The four-hole blasting model has the most abundant explosive cracks, and the resistivity generally increases up to 20 times. However, compaction still occurs between two large adjacent cracks, resulting in local resistivity reduction. For example, the width of the crack near SK-1 is 1.6 mm, the width of the lateral crack of SK-4 is 0.5–1.5 mm, and the resistivity of the region between SK-1 and SK-4 is reduced by about 5–10%.

Due to the low strength of the coal seam, local compaction is likely to occur when the coal is subjected to blasting dynamic pressure. The possible locations of the compaction area include the control area where the total S value is less than 0 and the area between two large cracks.

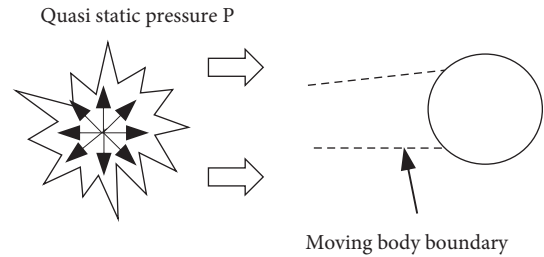


FIGURE 13: Control the movement boundary of coal inside the hole.

Outside the control area, the resistivity generally increases due to the existence of explosive cracks.

5. Discuss

Due to the difference in strength, the blasting form of the soft coal seam is different from that of the hard coal stratum. A large number of studies have been carried out on the formation mechanism of explosive cracks in China [8–16], which will not be described here. This section only analyzes the special cracking morphology of soft coal after blasting.

5.1. Local Coal Displacement. Soft coal has low strength and low impedance, and the effect of explosive gas is more obvious. The quasi-static pressure P generated by dynamic pressure and explosive gas expansion can cause displacement of coal between the blasting hole and the control hole, especially near the control hole. As shown in Figure 13. Coal displacement leads to the generation of shear cracks, whose width is the maximum in the whole control area. The quasi-static pressure P can be directly calculated by using the expansion pressure of detonation gas:

$$P = P_K \left(\frac{P_W}{P_K} \right)^{\gamma/K} \left(\frac{V_c}{V_0} \right)^\gamma. \quad (3)$$

In the formula, P_W is the average detonation pressure; P_K is the critical pressure. γ and K are adiabatic indexes and isentropic indexes respectively; V_c and V_0 are the volume of charge and the volume of blasting hole.

$$P_W = \frac{\rho_c D^2}{2(k+1)}. \quad (4)$$

In the formula, ρ_c and D are the density and detonation velocity of the explosive respectively.

The inner side of the control hole can be regarded as the free surface of the blasting hole, and then the action direction of the blasting energy can be controlled so that the inner side of the control hole presents the shape of the blasting funnel and pushes the coal forward.

When there are multiple blasting (control) holes in the coal seam, the stress waves reflect, diffract and superimpose on each interface (blasting crack surface, extraction hole wall, control hole wall, and blasting hole wall), and the effect on the coal becomes more complex, and the width of the crack is larger than that of the single-hole blasting model. The explosive gas has a more significant pushing effect on coal, especially on the inner side of the control hole.

Uneven distribution of circumferential tensile stress is generated at the edges of control holes or adjacent blasting holes [32], and the maximum tensile stress is generated at the inner and outer edges of the drilling line so that the detonation crack continues to expand along the line. The crack outside the control hole in the experimental model verifies this point, and the crack direction is consistent with the connection direction of the control hole and the blasting hole.

5.2. Local Compaction of Coal Seam. The resistivity inversion results show that the soft coal has been partially compacted after blasting. For example, in the single-hole blasting model, although there are cracks in the control area, it is difficult for the fine blasting cracks to cause damage to the whole control area. Under the action of blasting hole expansion, the control area instead presents a compacted state.

Resistivity is not only related to coal water content but also related to structural states, such as porosity change, deformation, and failure [33]. The pores in the compressed area of the coal seam are compacted, the conductive channels increase obviously, and the resistivity decreases. There may be two reasons for the compaction phenomenon in coal seams after blasting. One is the coal compression caused by the expansion of the blasting hole. Secondly, the opening of the crack leads to the compression of the coal on both sides of the crack plane, especially between the two crack planes.

The explosion gas has to scour and pushing effect on the soft coal, leading to the compaction of the coal, and its density will also increase [34], forming a local compaction area outside the blasting cavity. If the inner coal of the control hole is pushed and displacements occur, the

swelling and compaction effect of the blasting hole can be offset.

Space is needed for the generation of blasting crack, especially after the explosion gas enters into the crack, the gas expansion produces a driving force on the coal on both sides of the crack plane, and the coal is also compressed. If there are control holes near the cracks to provide spatial compensation, the coal compression can also be alleviated. Once there is no space compensation or low compensation degree of control hole around the crack, the degree of coal compression will inevitably increase. This is especially true in the area between the two cracks, which must find space to open by compressing the coal.

It can be seen that the key to solving the local compaction of coal seam lies in the spatial compensation degree of the control hole. Only by providing enough deformation space for blasting action can the permeability in the control area be effectively improved.

In the engineering practice of antireflection by blasting in the soft coal seam, the pure amount of gas extraction is usually large in a short time after blasting, and then the concentration of gas extraction decreases rapidly. The explosion crack in a soft coal seam is easy to close under the action of stress, and the expansion of the blasting hole also compacts the coal, so the analysis of the blasting antireflection effect in a soft coal seam should not only consider the explosion crack but should consider the change of coal structure comprehensively.

6. Conclusion

Model blasting experiments with blasting holes and control holes were carried out to analyze the blasting cracking characteristics of soft coal. The main conclusions are as follows:

- (1) After soft coal seam blasting, there will be three kinds of crack formation, such as explosion hole expansion, explosion crack formation, and control hole reduction, while explosion crack only appears outside the control area. There are crack and noncrack displacement modes between the blasting hole and control hole. Crack displacement leads to cracks with large width on the inner side of the control hole.
- (2) A quantitative comprehensive evaluation method of the antireflection effect is proposed, and the antireflection effect is comprehensively analyzed by using the area changes of explosion crack, control hole, and blasting hole. With the increase in the number of blasting holes, the positive reflection improvement effect is presented in the control area, and the width and fractal dimension of the explosion crack increase obviously, which can effectively improve the gas extraction efficiency of the coal seam.
- (3) The regional variation rule of coal resistivity before and after blasting was tested, and it was found that not all areas would be damaged obviously after

blasting, and the coal on both sides of the crack plane would be squeezed when the explosion crack was generated, leading to local compaction phenomenon.

Data Availability

The data used to support the findings of this study are included within the article.

Conflicts of Interest

The authors declare that they have no conflicts of interest.

Acknowledgments

The authors are grateful to the financial support from the National Natural Science Foundation of China (51704012 and 71971003).

References

- [1] H. L. Gu, M. Tao, W. Z. Cao, J. Zhou, and X. B. Li, "Dynamic fracture behaviour and evolution mechanism of soft coal with different porosities and water contents," *Theoretical and Applied Fracture Mechanics*, vol. 103, no. 103, Article ID 102265, 2019.
- [2] Y. Xue, J. Liu, P. G. Ranjith, Z. Z. Zhang, F. Gao, and S. H. Wang, "Experimental investigation on the nonlinear characteristics of energy evolution and failure characteristics of coal under different gas pressures," *Bulletin of Engineering Geology and the Environment*, vol. 81, no. 1, p. 38, 2022.
- [3] R. L. Zhang, Z. J. Chen, and J. W. Chen, "Experimental research on the variational characteristics of vertical stress of soft coal seam in front of mining face," *Safety Science*, vol. 50, no. 4, pp. 723–727, 2012.
- [4] H. D. Liang, P. F. Guo, D. J. Sun, K. K. Ye, B. P. Zou, and Y. D. Yuan, "A study on crack propagation and stress wave propagation in different blasting modes of shaped energy blasting," *Journal of Vibration and Shock*, vol. 39, no. 4, pp. 157–164, 2020.
- [5] D. Y. Guo, C. Zhang, K. Li, and T. G. Zhu, "Mechanism of millisecond delay detonation on coal cracking under deep - hole cumulative blasting in soft and low permeability coal seam," *Journal of China Coal Society*, vol. 46, no. 8, pp. 2583–2592, 2021.
- [6] Z. W. Ye, M. Chen, T. Li, W. B. Lu, and P. Yan, "A simplified method for calculating peak pressure of borehole wall under water-coupling contour blasting," *Rock and Soil Mechanics*, vol. 46, no. 10, pp. 2808–2818, 2021.
- [7] B. W. Xia, Y. G. Gao, C. W. Liu, C. N. Ou, Z. Y. Peng, and L. Liu, "Experimental study on rock-breaking load in slot-hydraulic blasting," *Chinese Journal of Engineering*, vol. 42, no. 9, pp. 1130–1138, 2020.
- [8] W. Yuan, W. Wang, X. B. Su, L. Wen, and J. F. Chang, "Experimental and numerical study on the effect of water-decoupling charge structure on the attenuation of blasting stress," *International Journal of Rock Mechanics and Mining Sciences*, vol. 2019, Article ID 104133, 124 pages, 2019.
- [9] Y. Z. Yang, Z. S. Shao, X. F. Xiong, and J. F. Mi, "Comparison of radial and axial uncoupled charge in rock blasting," *Blasting*, vol. 35, no. 04, pp. 26–33+146, 2018.
- [10] Q. Zhu, M. Chen, B. X. Zheng, and P. Yan, "Distribution and control technology of rock damage induced by air-deck charge presplitting blasting," *Chinese Journal of Rock Mechanics and Engineering*, vol. 35, no. S1, pp. 2758–2765, 2016.
- [11] G. L. Yang, S. J. Cheng, P. Wang, X. H. Li, and Y. G. Yan, "Blasting experiment of axial uncoupled charge for slotted tube," *Explosion and Shock Waves*, vol. 37, no. 01, pp. 134–139, 2017.
- [12] Z. R. Zhang, J. J. Zuo, and Y. X. Guo, "Crack propagation behavior of empty hole defects under blast load," *Journal of Vibration and Shock*, vol. 39, no. 3, pp. 111–119, 2020.
- [13] M. Li, X. P. Lai, J. G. Zhang, S. S. Xiao, L. M. Zhang, and Y. H. T, "Blast-casting mechanism and parameter optimization of a benched deep-hole in an opencast coal mine," *Shock and Vibration*, vol. 2020, no. 4, pp. 1–11, Article ID 1396483, 2020.
- [14] H. B. Chu, X. L. Yang, W. M. Liang, and Y. Q. Yu, "Study on the damage-crack process and mechanism of coal blasting," *Journal of Mining and Safety Engineering*, vol. 35, no. 2, pp. 410–414, 2018.
- [15] X. L. Li, S. J. Wang, S. Zhao, M. Liu, and H. Liu, "Study on in situ stress distribution law of the deep mine: taking linyi mining area as an example," *Advances in Materials Science and Engineering*, vol. 2021, no. 4, pp. 1–11, Article ID 5594181, 2021.
- [16] R. S. Yang, C. X. Ding, Y. B. Wang, and C. Chen, "Action-effect study of medium under loading of explosion stress wave and explosion gas," *Chinese Journal of Rock Mechanics and Engineering*, vol. 35, no. 02, pp. 3501–3506, 2016.
- [17] H. L. Fei and C. C. Hong, "Study on crushed and crack zone range under combined action of stress and detonation gas," *Blasting*, vol. 34, no. 1, pp. 33–36, 2017.
- [18] M. Fakhimi and A. Fakhimi, "Numerical study of contributions of shock wave and gas penetration toward induced rock damage during blasting," *Computational Particle Mechanics*, vol. 2, no. 2, pp. 197–208, 2015.
- [19] C. J. Pu, X. Yang, H. Zhao et al., "Numerical study on crack propagation under explosive loads," *Acta Mechanica Sinica*, vol. 38, no. 1, Article ID 421376, 2022.
- [20] X. L. Li, S. J. Chen, Q. M. Zhang, G. Xin, and F. Feng, "Research on theory, simulation and measurement of stress behavior under regenerated roof condition," *Geomechanics and Engineering*, vol. 26, no. 1, pp. 49–61, 2021.
- [21] H. Y. Liu, B. Y. Zhang, X. L. Li et al., "Research on roof damage mechanism and control technology of gob-side entry retaining under close distance gob," *Engineering Failure Analysis*, vol. 138, no. 5, Article ID 106331, 2022.
- [22] C. L. He and J. Yang, "Experimental and numerical investigations of dynamic failure process in rock under blast loading," *Tunnelling and Underground Space Technology*, vol. 83, pp. 552–564, 2019.
- [23] J. Y. Feng, X. H. Liu, and Z. Q. Yu, "Numerical simulation study on the mining-induced fracture evolution of steep coal seam," *Journal of China Coal Society*, vol. 42, no. 8, pp. 1971–1978, 2017.
- [24] X. Hui, F. S. Ma, J. M. Xu, and J. Guo, "Study on statistical damage constitutive model for rocks considering length and occurrence distribution of joint fissures," *Chinese Journal of Rock Mechanics and Engineering*, vol. 36, no. S1, pp. 3233–3238, 2017.
- [25] S. M. Liu, X. L. Li, D. K. Wang, and D. M. Zhang, "Investigations on the mechanism of the microstructural evolution of different coal ranks under liquid nitrogen cold soaking,"

- Energy Sources, Part A: Recovery, Utilization, and Environmental Effects*, pp. 1–17, 2020.
- [26] H. Sun, X. L. Liu, and J. B. Zhu, “Correlational fractal characterisation of stress and acoustic emission during coal and rock failure under multilevel dynamic loading,” *International Journal of Rock Mechanics and Mining Sciences*, vol. 117, pp. 1–10, 2019.
 - [27] D. P. DeLellis, N. A. Mecholsky, J. J. Mecholsky, and G. D. Quinn, “A fractal analysis of crack branching in borosilicate glass,” *Journal of the American Ceramic Society*, vol. 103, no. 9, pp. 5283–5290, 2020.
 - [28] J. Y. Chen, H. Zhao, and M. H. Zhao, “Image processing and multi-fractal characteristics of fly ash particles,” *Journal of Hunan University*, vol. 48, no. 11, pp. 205–214, 2021.
 - [29] S. D. Liu, J. Liu, J. Qi, Y. Cao, and R. Q. Lv, “Applied technologies and new advances of parallel electrical method in mining geophysics,” *Journal of China Coal Society*, vol. 44, no. 8, pp. 2336–2345, 2019.
 - [30] Z. H. Shang, X. J. Xian, G. P. Li et al., “Application of network concurrent electric method in coal face roof “two zones” height detection,” *Coal Geology of China*, vol. 34, no. 6, pp. 73–79, 2022.
 - [31] S. C. Zhang, Z. G. Liu, J. Liu, Z. Q. Li, and K. Gao, “Tests for control hole’s enhanced permeability mechanism under blasting load,” *Journal of Vibration and Shock*, vol. 36, no. 24, pp. 213–219, 2017.
 - [32] K. Man and X. L. Liu, “The effect of surrounding empty holes on the blasting velocity and damaged zones,” *Engineering Mechanics*, vol. 37, no. 11, pp. 127–134, 2020.
 - [33] T. Y. Qi, G. R. Feng, Y. X. Guo, J. Guo, and Y. J. Zhang, “Effects of fine gangue on strength, resistivity, and microscopic properties of cemented coal gangue backfill for coal mining,” *Shock and Vibration*, vol. 2015, pp. 1–11, Article ID 752678, 2015.
 - [34] Y. L. Zhang, N. X. Sun, Y. Mao et al., “Study on the influence mechanism of weak interlayer on tunnel smooth blasting effect,” *Journal of Railway Science and Engineering*, vol. 17, no. 1, pp. 148–158, 2020.